



STRUCTURAL
BIOLOGY

Volume 72 (2016)

Supporting information for article:

**The supramolecular structure of bone: X-ray scattering analysis
and lateral structure modeling**

**Hong-Wen Zhou, Christian Burger, Hao Wang, Benjamin S. Hsiao, Benjamin
Chu and Lila Graham**

I. BONE AS AN ORGAN

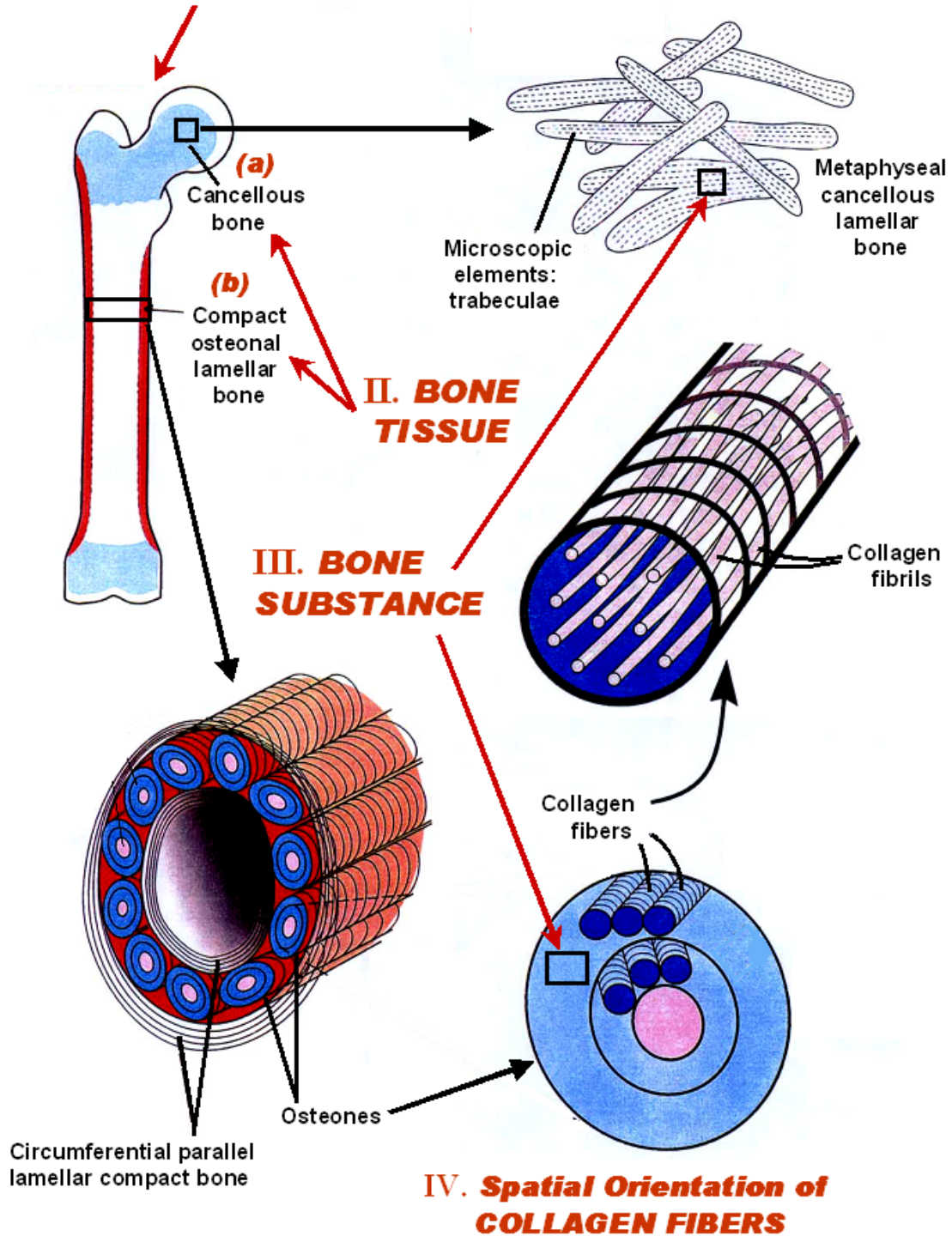


Figure S1 The hierarchical structure of bone. Collagen fibers (center right) are composed of fibrils, the subject of the present study (Adapted from (Glimcher, 1998)).

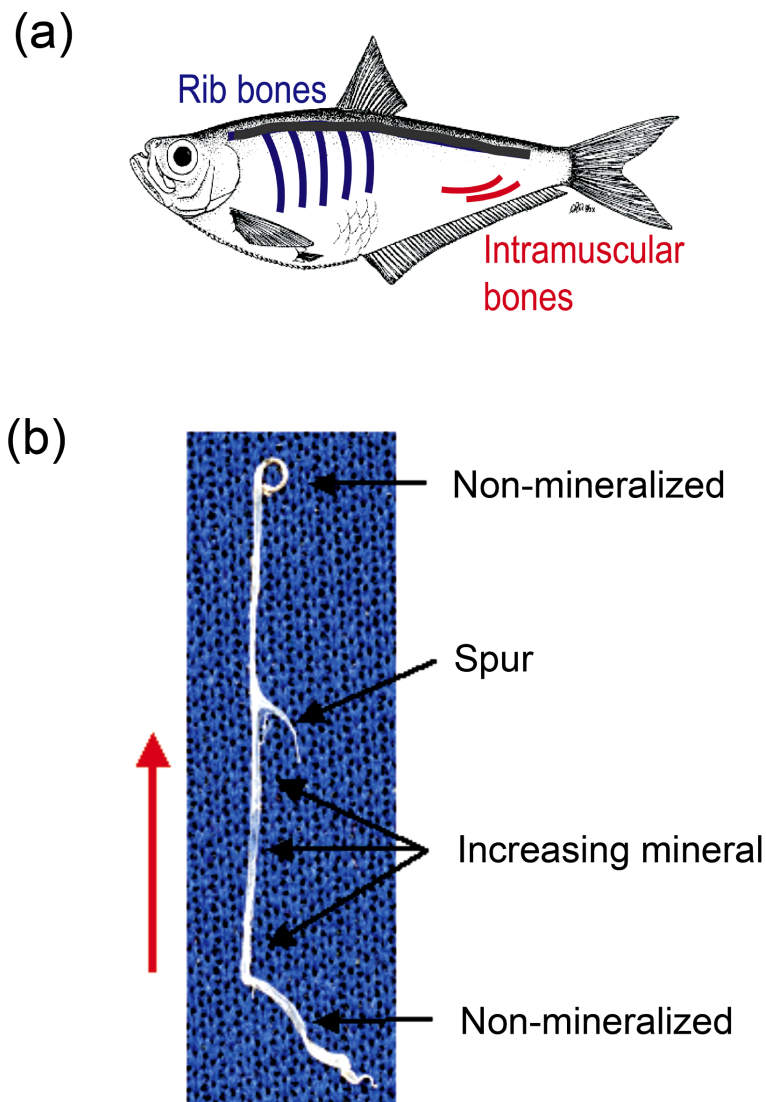


Figure S2 Intramuscular fish bone. (a) Schematic illustration of the anatomical location of intramuscular bones. In zebrafish skeletal preparations, they have been visualized by staining (Connolly & Yelick, 2010). (b) Photo of a herring bone (*C. harengus*) on a blue background. Typically, adult herring intramuscular bones are about 2-4 cm in length and 0.5–2 mm in width. The twisted ends of the bones are non-mineralized collagen. In the area below the spur, the direction of increasing mineralization is indicated by the red arrow (Burger *et al.*, 2008). This region is predominantly composed of collagen fibrils oriented roughly parallel to the axis of the bone (Lee & Glimcher, 1991). Herring bone mechanical characteristics can be described as similar to string at the non-mineralized ends, and similar to a toothpick in the mineralized areas. Nanoindentation studies of herring bone found that the indentation modulus generally (in central locations) increased with degree of mineralization. The reported modulus ranged from about 3.5 to 20 Gpa (Rho *et al.*, 2001). The function of intramuscular bones is not well understood.

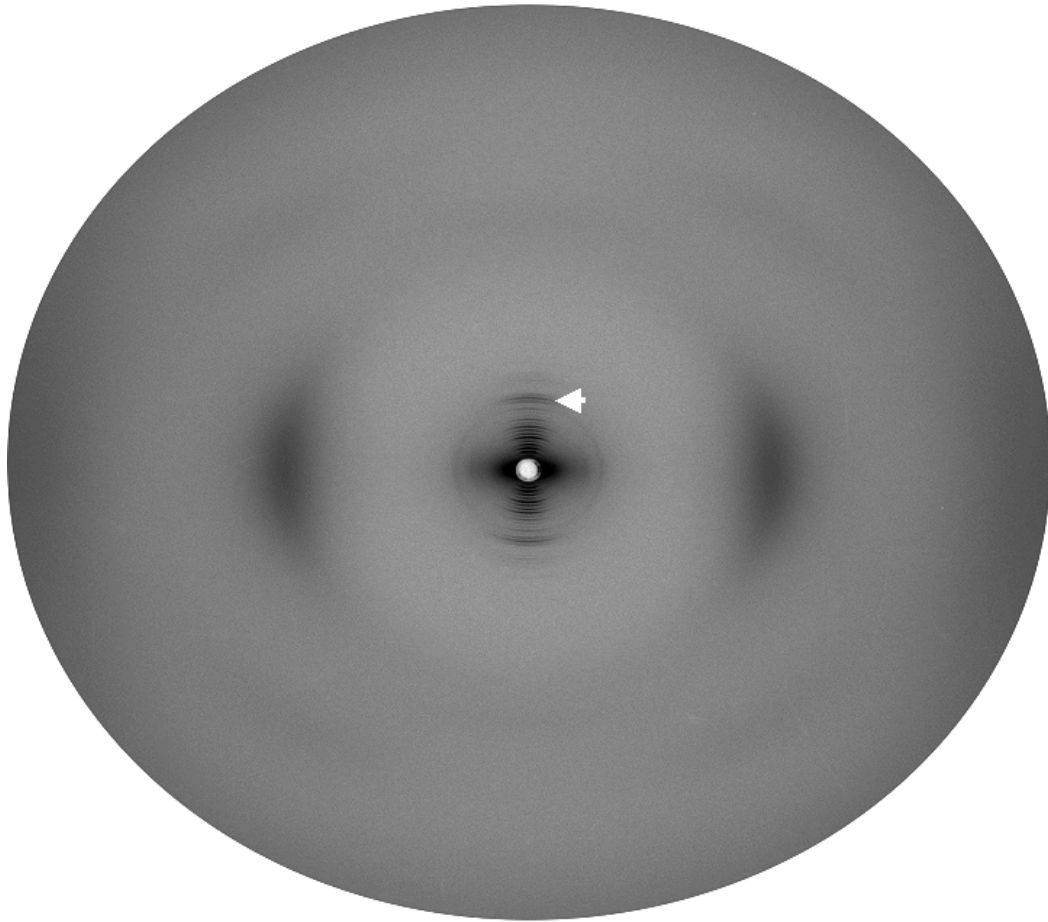


Figure S3 SAXS pattern for pre-mineralized intramuscular shad bone. Two equatorial Bragg reflections/row lines are observed at 4.76(5) nm and 3.68(1) nm and the intermolecular interference maximum is located at about 1.10 nm. The overall equatorial scattering features for shad bone are similar to those for herring bone, indicating that collagen fibrils in shad bone have a similar lateral packing structure to that shown in However, fewer equatorial reflections are observed and their intensities are weaker, suggesting the lateral packing in shad bone fibrils is less ordered. The arrow indicates the 20th order meridional reflection. The longitudinal periodicity is 65.1(1) nm.

Table S1 “Diameters” of the collagen triple helix and Smith five-stranded microfibril.

Type	Diameter (nm)	Techniques	Remarks
Triple Helix:			
Reconstituted steer skin collagen	1.18	XRD	Equivalent diameter (Katz & Li, 1973)
	1.25	XRD	Contact diameter (Katz & Li, 1973)
Turkey leg tendon collagen	1.19	XRD	Effective repulsion diameter (Fratzl <i>et al.</i> , 1993)
RTT collagen	1.18	XRD	Effective repulsion diameter (Woodhead-Galloway & Machin, 1976)
Ala substituted (Gly-Pro-Hyp) ₁₀	1.0	XRD	No long side chains (Bella <i>et al.</i> , 1994)
[(Gly-Pro-Pro) ₁₀] ₃	1.0	XRD	No long side chains (Berisio <i>et al.</i> , 2002)
(Gly-Pro-Hyp) ₁₂	1.26	Energy-minimized computational model	No long side chains (Chen <i>et al.</i> , 1991)
Microfibril:			
(Gly-Pro-Hyp) ₁₂	3.20	Energy-minimized computational model	No long side chains (Chen <i>et al.</i> , 1991)
Bovine type I collagen, segment	2.87 ~ 3.43	Energy-minimized computational model	Backbone (Brown <i>et al.</i> , 1997)
	3.20 ~ 3.55	Energy-minimized computational model	With side chains (Brown <i>et al.</i> , 1997)

Discussion S1 Implications of a spatially discrete microfibril model for bone collagen post-translational modifications (PTMs).

S1.1 General considerations

The function of most bone collagen PTMs is to structurally stabilize and strengthen the bone organic matrix. Normal bone requires collagen molecules that are both covalently and non-covalently bound to their neighbors inside a fibril. A covalent crosslinking model for bone must first be consistent with established peptide chain loci for crosslinks in type 1 collagen (Eyre & Weis, 2013, Knott & Bailey, 1998, Yamauchi & Sricholpech, 2012). Figure S4b shows a Smith microfibril, as originally represented (Smith, 1968), with appropriate loci for crosslinks. These links would create four “strings” of covalently bound collagen molecules, giving the microfibrils longitudinal tensile strength (see also Fig. S5c). A bone fibril would further require lateral linkages between microfibrils (Fig. S4c). In the absence of such links, a fibril could more easily fall apart, analogous to a handful of dry spaghetti. The well-established chemical, thermal, and mechanical stability of the bone collagen matrix would appear to require intermicrofibrillar crosslinking, and in fact, as discussed in section S1.3, there is evidence to indicate that it does exist. For reasons explained in the same section, different crosslinking structures would be suitable for different intermicrofibrillar crosslinking sites (Fig. S4c).

S1.2 Collagen crosslinking in mineralized tissues

S1.2a Crosslink structures and biosynthesis

The chemistry of collagen crosslinking has been reviewed (Eyre & Weis, 2013, Knott & Bailey, 1998, Yamauchi & Sricholpech, 2012). In mineralized tissues the predominant crosslink structures fall into two categories: dipeptidyl crosslinks (linking two peptide chains) and tripeptidyl crosslinks (linking three chains). The dipeptidyls are primarily ketoamines (Table S2, first row). Tripeptidyls include both pyrroles and hydroxypyridiniums (Hpyds) (Table S2, second and third rows, respectively). All of these crosslinks can have hydroxyl or glycosyl modifications at the indicated “R” positions. Intracellular steps in the biosynthesis of bone collagen include co-translational hydroxylation of specific lysine residue side chains ($\sim\sim(\text{CHOH})\text{-CH}_2\text{NH}_2$), which can be followed by attachment of a glycosyl residue to the hydroxyl group. Extracellularly, specific lysine or hydroxylysine (Hyl) residues are oxidatively deaminated by the enzyme lysyl oxidase to produce ϵ aldehydes ($\sim\sim(\text{CHOH})\text{-CH=O}$). The aldehydes react rapidly and spontaneously with the ϵ amines of lysine (or modified lysine) residues in adjacent collagen molecules to produce Schiff base crosslinks. Schiff bases derived from oxidized Hyl ($\sim\sim(\text{CHOH})\text{-CH=N-CH}_2\text{-CHR}\sim\sim$) can undergo spontaneous Amadori rearrangement to form ketoamines (Table S2, first row). The same residues, at the same loci, that are involved in ketoamine formation are ultimately involved in tripeptidyl formation. As tissues mature, ketoamine levels decline and tripeptidyl levels increase. For these reasons, ketoamines appear to be precursors of tripeptidyls, although the mechanistic details of this conversion are unclear. Tripeptidyls form spontaneously, but extremely slowly compared to the spontaneous formation of Schiff bases.

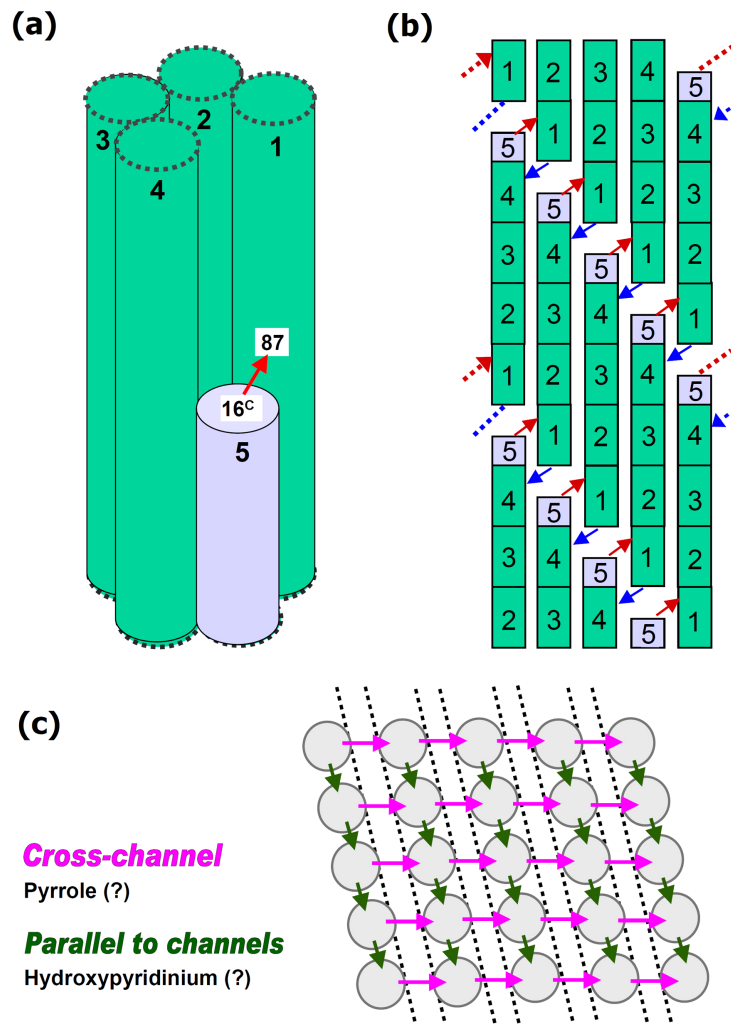
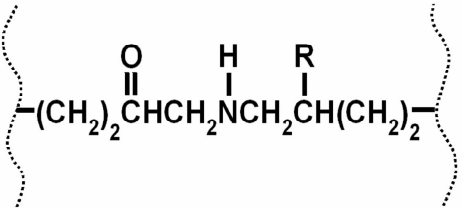
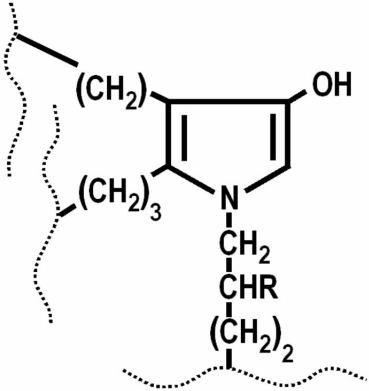
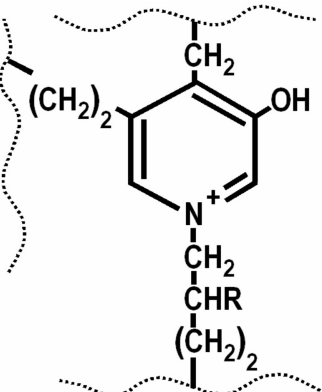
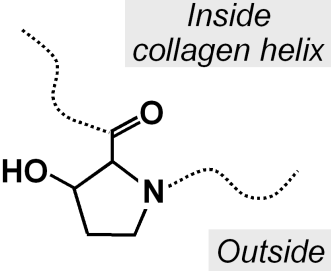


Figure S4 Potential collagen crosslinking for a pentagonal, quarter-staggered microfibril based on reported crosslink loci in type I collagen (see text). (a) Schematic three-dimensional illustration of a potential crosslinking site. A C-terminal telopeptide residue at position 16^C links to a helical residue at position 87 on an adjacent molecule. (b) Schematic two-dimensional illustration of crosslinking in a Smith-type microfibril that has been “unrolled” for clarity (Smith, 1968). Red arrows represent potential links of telopeptide residues at position 16^C (on α 1 chains) with helical residues at position 87 (α 1 or α 2). Blue arrows represent potential links of telopeptide residues at position 9^N (α 1) or 5^N (α 2) with helical residues at position 930 (α 1) or 933 (α 2). (c) Illustration of two possible orientations of intermicrofibrillar crosslinks (see Fig. 8a).

Table S2 Collagen post-translational modifications (PTMs) found in mineralized tissues and their proposed functions. Dotted lines represent collagen peptide chains.

Structure (R = H, OH, or O-glycosyl)	Type, tissue specificity, proposed function
	<p>Dipeptidyl (mostly ketoamine) crosslinks – Mature mineralized tissues have much more of this PTM than other mature tissues. After microfibril assembly, they would link collagen molecules into four strings (Fig. S4b, S5c). Those with O-Gal-Glc tags (Terajima <i>et al.</i>, 2014) would mostly remain as dipeptidyls to preserve microfibril longitudinal tensile strength; those with O-Gal tags could potentially react to form tripeptidyls (below).</p>
	<p>Pyrrole (tripeptidyl) crosslinks – With the exception of some high-load tendons, only mineralized tissues contain this PTM (Eyre & Weis, 2013, Knott & Bailey, 1998, Yamauchi & Sricholpech, 2012). In bone, its glycosyl tag is mainly O-Gal (Terajima <i>et al.</i>, 2014). The charge neutrality of pyrroles would allow them to link microfibrils (to provide lateral tensile strength for fibrils) at cross-channel sites in close proximity to mineral (Figs. S4c, S6, S7).</p>
	<p>Hydroxypyridinium (Hpyd) (tripeptidyl) crosslinks – Generally, bone has a lower content of this PTM than cartilage, ligament, or tendon (Eyre <i>et al.</i>, 1984). There are no Hpyds in skin or cornea (Eyre & Weis, 2013, Knott & Bailey, 1998, Yamauchi & Sricholpech, 2012). Its glycosyl tag is primarily O-Gal, as is the case for pyrroles (Terajima <i>et al.</i>, 2014). Hpyds would also link microfibrils. They would be preferred in sites where their charge is not a problem, since they are more chemically stable than pyrroles.</p>
	<p>3-Hydroxylated proline (3Hyp) – Normal bone requires high occupancy at position $\alpha 1(I)986$ by this PTM; its evolutionary appearance at this locus closely preceded the appearance of vertebrates (Eyre & Weis, 2013). 3Hyp would facilitate axial alignment of molecules for microfibril assembly and provide lateral microfibril stability, analogous to the role of 4Hyp in lateral stabilization of triple-helical collagen molecules.</p>

S1.2b The unexplained uniqueness of mineralized tissue crosslinking

As soft tissues mature and age, ketoamines generally decline to nearly undetectable levels, while in bone they remain in substantial quantities. Pyrroles occur almost exclusively in mineralized tissues (Eyre & Weis, 2013; Knott & Bailey, 1998). In mature bone, Hpyd levels are much lower than those commonly found in cartilage, tendon, or ligament (Eyre *et al.*, 1984). The Hyl content of bone is about half that of cartilage, resulting in lower levels of crosslink hydroxylation (Eyre & Weis, 2013). This unique pattern of crosslink types and quantities can be explained (section S1.3b) with the benefit of some insight into the molecular packing structure of bone collagen.

S1.3 Bone fibril biosynthesis

S1.3a Microfibrils

As collagen chains are synthesized, certain proline residues are hydroxylated in a tissue-specific manner. Completed chains are assembled into triple-stranded procollagen molecules. After procollagen secretion and enzymatic removal of the N- and C-terminal propeptides, the remaining molecule consists of a lengthy triple helix and short non-helical N- and C-terminal telopeptides (reviewed in (Yamauchi & Sricholpech, 2012)). The triple helix (for type I collagen, two $\alpha 1(I)$ chains and one $\alpha 2(I)$) is stabilized primarily by hydrogen bonding involving 4-hydroxylated proline (4Hyp) (reviewed in (Brodsky & Persikov, 2005)). Although soft tissue collagen molecules can spontaneously assemble into D-periodic fibrils, the biosynthetic pathway for a bone microfibril would be more complex. Residues of 3-hydroxylated proline (3Hyp) (Table S2, fourth row) are distributed differently in the type I collagen chains of bone and tendon (Eyre *et al.*, 2011). In human bone, absence of 3Hyp at position $\alpha 1(I)986$ is associated with brittle bone disease (Eyre & Weis, 2013). Analogous to the role of 4Hyp in stabilizing the collagen triple helix, 3Hyp in bone may contribute to the lateral stability of the microfibril helix. Fig. S5b shows 3Hyp residues occurring in D-periodic pairs along the microfibril axis (Eyre & Weis, 2013). The position of the $\alpha 1(I)986$ residue near the C-terminal suggests that it might also assist in axial alignment of collagen molecules during microfibril assembly, which would then proceed from the C- to N-terminal direction, as occurs for a collagen triple helix (Brodsky & Shah, 1995). Smith microfibrils would be good substrates for lysyl oxidase, according to a current model (Nagan & Kagan, 1994). The positions of crosslinking sites in a microfibril would allow formation of dipeptidyls (Fig. S5c).

S1.3b Mineralized fibrils

Fig. S6 illustrates steps that would be required for assembly of a mineralized fibril. Assembled microfibrils are shown in a parallel configuration, consistent with loci of residues contributing to tripeptidyl crosslinks, and the requirement for gap zones to be aligned to form channels. A premineralized fibril would be held together by some currently uncharacterized binder/spacer molecules, or possibly by specifically configured telopeptides. In (b) calcium, phosphate, and other ions diffuse through the channels into the fibril interior to form mineral crystals. The nature of the intermicrofibrillar crosslinking in (c) is indicated by the finding that additional Hpyds can form in a bone matrix from which mineral has been removed (Eyre, 1981). These crosslinks must be intermicrofibrillar (see Fig. 8a). In a

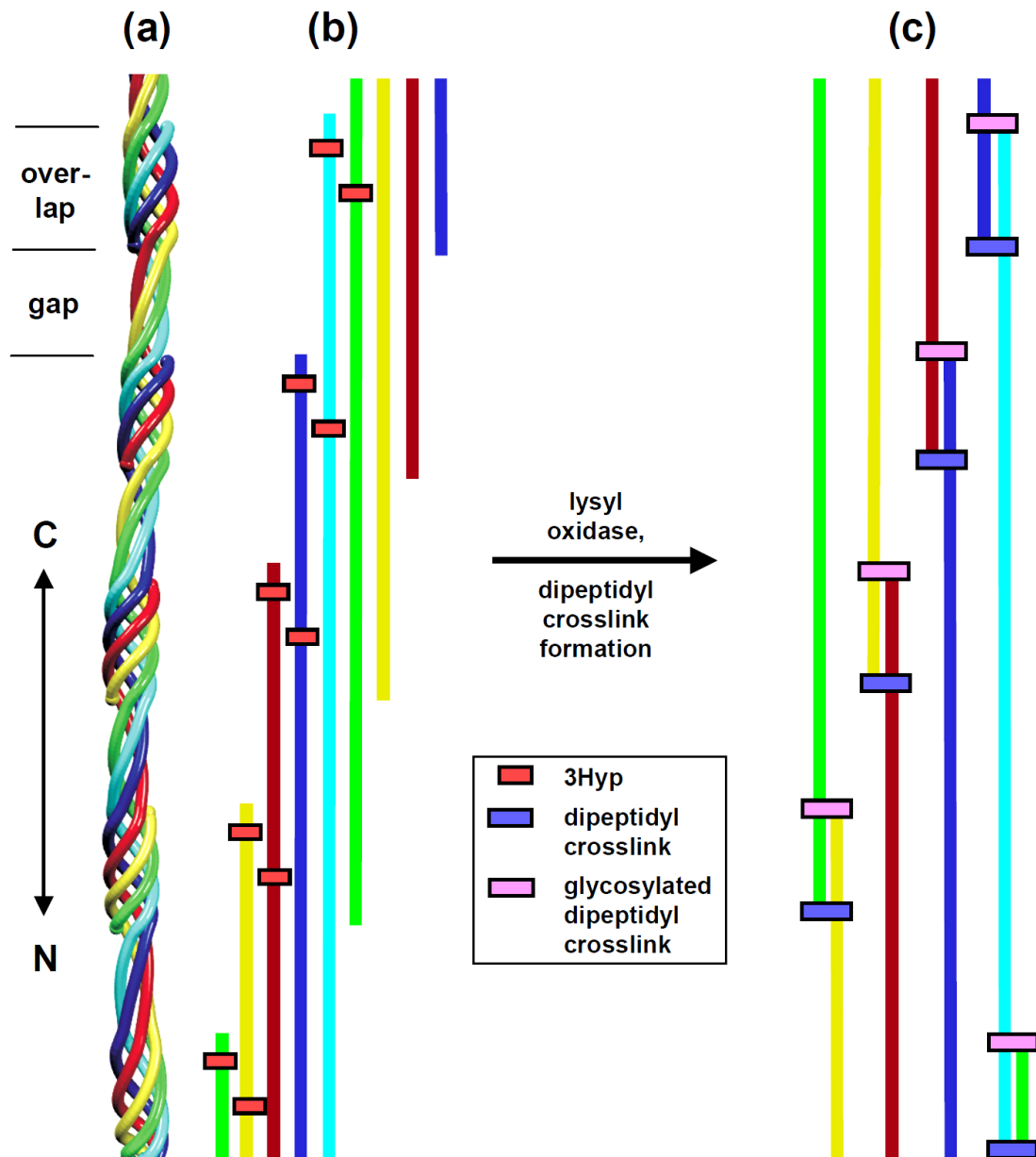


Figure S5 Proposed microfibril assembly and stabilization. Colored lines represent collagen molecules. Schematic illustrations of (a) a segment of a microfibril in 3D format; (b) the same microfibril segment in “unrolled” 2D format, laid out to show the positions of 3Hyp residues (orange bars); (c) the same segment in “unrolled” 2D laid out to show positions which can be occupied by dipeptidyl crosslinks (pink and purple bars). N- and C-terminal directions are indicated at left. In (b), the orange bar near the C-terminal end of each molecule represents proline at position $\alpha 1(I)986$ that is about 94% 3-hydroxylated in human bone; the lower orange bar is position $\alpha 2(I)707$, where proline is about 18% 3-hydroxylated (Eyre *et al.*, 2011). Normal bone has a critical requirement for the $\alpha 1$ 3Hyp (Eyre & Weis, 2013). In (c), dipeptidyl crosslinks stabilize microfibrils longitudinally (provide longitudinal tensile strength) by forming four continuous strings of covalently linked collagen molecules. (In descriptions of a Smith microfibril, the term “five-stranded” refers to the number of molecules in the overlap zone (shown at left)). 3Hyp is omitted in (c) for clarity. Loci for glycosylated crosslinks are shown as determined for ~ 2-yr-old bovine femur (Terajima *et al.*, 2014).

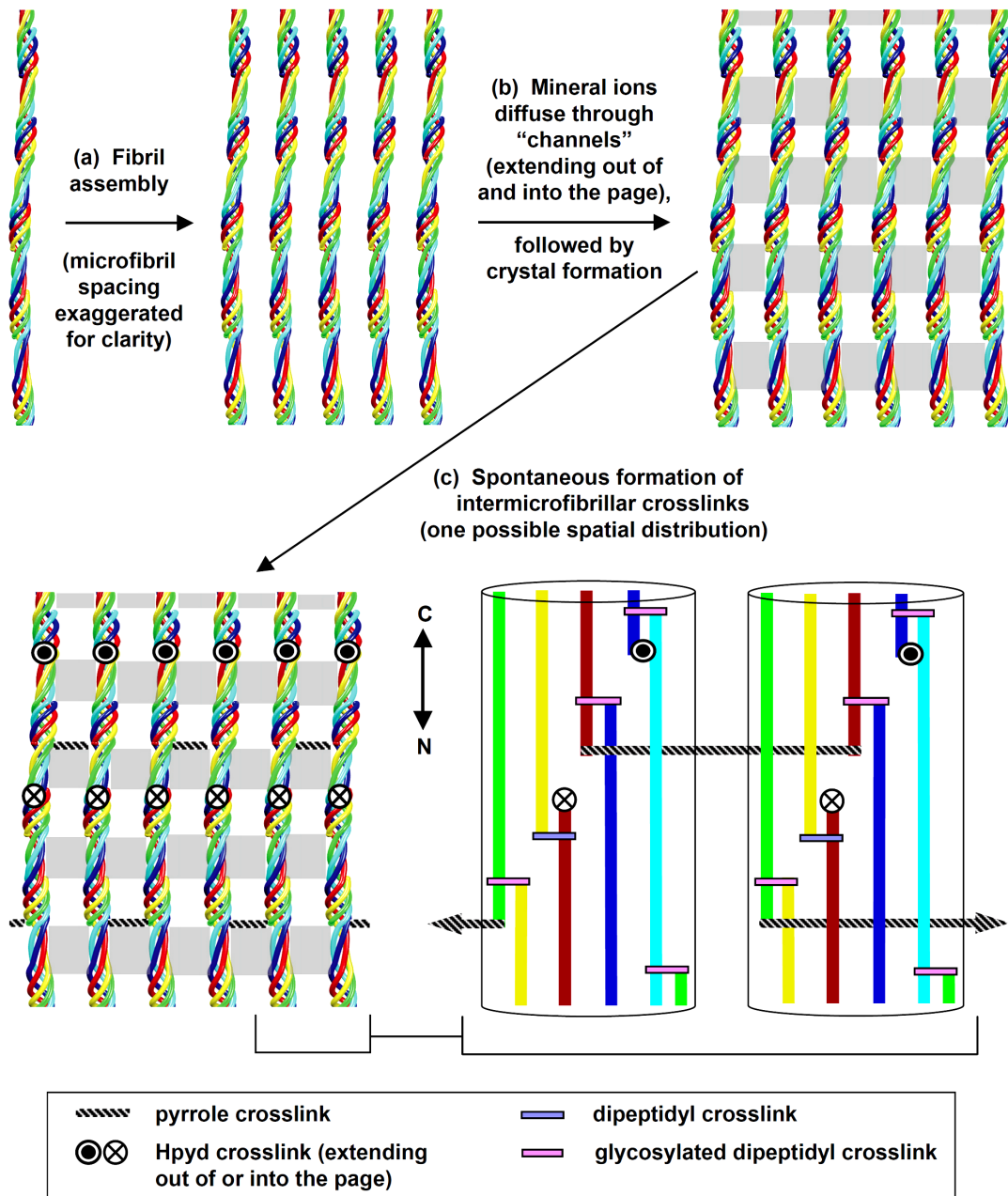


Figure S6 Proposed mineralized fibril assembly and stabilization. Colored lines represent collagen molecules. Schematic illustrations of: (a) fibril assembly, (b) fibril mineralization, and (c) spontaneous formation of intermicrofibrillar crosslinks. Gray areas in (b) indicate spaces available for mineral crystal formation. In (c), potential sites for intermicrofibrillar crosslinking are shown as crosshatched lines (pyrroles) and circles (Hpyds). This crosslinking scheme is one possibility consistent with quantities and loci of crosslinks in mature human cortical bone, and glycosylation sites in bovine bone (Hanson & Eyre, 1996, Terajima *et al.*, 2014). N- and C-terminal directions are indicated. Hpyds would extend parallel to the channels (Fig. S4c); i. e., out of and into the page. In the lower right is an expanded view of the two right-hand microfibrils showing intermolecular connections. Collagen molecules beneath crosshatched lines are linked by pyrroles. Molecules beneath circles are linked by Hpyds. C-terminal tripeptidyls are mostly glycosylated (Hanson & Eyre, 1996, Terajima *et al.*, 2014)

normal bone matrix, cross-channel sites may be more suitable for pyrroles (Fig. S4c). Since Hpyds have an irreversible positive charge, the proximity of apatite crystals could create an energetically unfavorable environment for Hpyd formation. Crosslinking sites parallel to the channels would be compatible with Hpyds, where they would be preferred since they are more chemically stable than pyrroles. This arrangement is consistent with a specific mineralized tissue requirement for pyrroles, and with roughly equal numbers of pyrroles and Hpyds (Hanson & Eyre, 1996). The relatively low levels of Hyl in bone may be due to the fact that pyrroles, compared to Hpyds, require a larger precursor pool of non-hydroxylated lysine.

Hpyds are too small to span the distance between microfibrils (Mechanic *et al.*, 1985) (see Fig. S7, lower right). A crosslinking mechanism is required that results in bridging the intermicrofibrillar gap. It must also be consistent with a precursor/product relationship for dipeptidyls and tripeptidyls. It has been suggested that certain histidine residues may play a role in tripeptidyl crosslink formation (Hanson & Eyre, 1996). Since the reverse Amadori rearrangement for ketoamines derived from peptidyl lysine occurs at a higher rate in tris (an amine buffer) compared to phosphate (Acharya & Sussman, 1984), this reaction may be catalyzed by amines, possibly including histidine. For a ketoamine crosslink, one product (after Schiff base hydrolysis) would be a free peptidyl aldehyde, which would be more reactive than the crosslink, and it would be located on an unlinked telopeptide that could span the intermicrofibrillar gap.

In Figs. S5c, S6c, and S7, distributions of crosslinks between N- and C-terminal sites are consistent with published data (Hanson & Eyre, 1996, Terajima *et al.*, 2014). Tripeptidyl crosslink loci were determined using human bone (Hanson & Eyre, 1996); glycosylation analysis was done with bovine bone (Terajima *et al.*, 2014). To our knowledge, there is currently no information on collagen crosslinking in fish bone. However, crosslinking chemistry and loci have evidently been conserved as vertebrate species have evolved. Lysyl oxidase consensus sequences (Nagan & Kagan, 1994) appear at appropriate collagen chain loci for both trout and zebrafish (Dubois *et al.*, 2002, Fisher *et al.*, 2003, Saito *et al.*, 2001, Strausberg *et al.*, 2002).

To conform to reported crosslink quantities in human bone (Eyre *et al.*, 1988), the model described here specifies a level of two dipeptidyls per molecule of collagen in newly formed microfibrils. In Fig. S5c, each collagen molecule is crosslinked to two others by four dipeptidyls. Each dipeptidyl is linked to two molecules, so each molecule “owns” one half of four dipeptidyls, or two crosslinks per molecule. As a fibril matures, tripeptidyls form, consuming two dipeptidyls each. Thus, tripeptidyl crosslinks are associated by origin with four molecules per crosslink; three of these molecules become linked by the tripeptidyl, one does not. If each collagen molecule is associated (by origin) with one pyrrole and one Hpyd, each molecule would “own” one quarter of a pyrrole and one quarter of a Hpyd, and levels for each tripeptidyl would be 0.25 mol crosslinks/mol collagen. These quantities are in rough agreement with the reported amount of Hpyds in 25-yr-old human cortical bone (0.29 mol/mol collagen) with an estimated equal amount of pyrroles (Hanson & Eyre, 1996). If half of the original dipeptidyls are consumed to form tripeptidyls (see Fig. S7 compared to Fig. S5c), the resulting dipeptidyl level would be 1.0 mol dipeptidyls/mol collagen, as found for 20-30 yr human cortical bone (Eyre *et al.*, 1988). Some dipeptidyls may be protected from conversion to

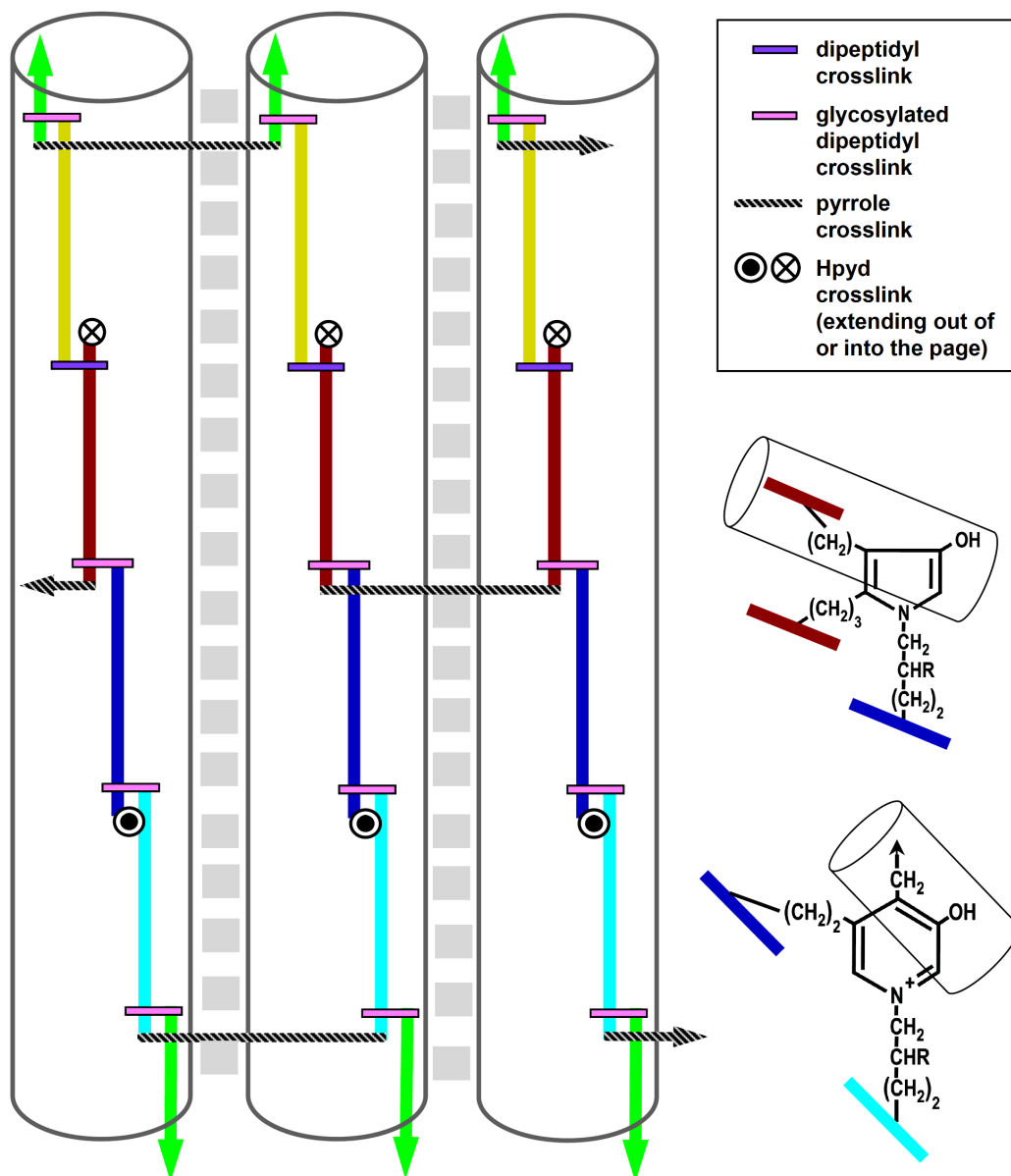


Figure S7 An extended view of the crosslinking scheme in Fig. S6c. Three linked strings of collagen molecules with the same axial stagger are illustrated, each in a separate microfibril. Individual microfibrils are composed of four strings. For clarity, only one string in each microfibril is shown. On the right, the pyrrole (upper) and Hpyd (lower) crosslinks connect collagen molecules indicated by the colored lines. The pyrrole links the center and right-hand microfibrils. The Hpyd links the right-hand microfibril with a microfibril located above the page. Cylinders represent one of two microfibrils connected by each crosslink, and indicate the microfibrillar origins of different parts of the crosslinking structures. Each crosslink is located near one of the two linked microfibrils. The intermicrofibrillar distance is spanned by a portion of a telopeptide (see text). Crosslink quantities (total dipeptidyls and total tripeptidyls) are consistent with reported values for human cortical bone at about 20-30 years of age (Eyre *et al.*, 1988, Hanson & Eyre, 1996). The ratio of Hpyds to pyrroles shown here is 1.0, as estimated for 25-yr-old human cortical bone (Hanson & Eyre, 1996). This ratio may vary among species, ages, anatomical sites, disease states, and/or individual subjects (Knott *et al.*, 1995, Bailey *et al.*, 1999, Banse *et al.*, 2002).

tripeptidyls by glycosylation (Terajima *et al.*, 2014). The interaction of a histidine residue with a ketoamine could be blocked to some degree by a bulky sugar moiety attached to the crosslink, thereby reducing the rate of the reverse Amadori rearrangement and subsequent tripeptidyl formation. Preservation of a ketoamine would be favored by glycosylation, lack of histidine near the helical crosslinking site, and/or obstruction of tripeptidyl formation by mineral. For the scheme illustrated in Fig. S7, there are positions where dipeptidyl links must remain intact to avoid breaking strings. These dipeptidyls amount to about half of the total, or 0.5 mol/mol collagen in adult human cortical bone. The relatively high dipeptidyl level in mature bone can thus be accounted for based on this model. A dipeptidyl range of 0.5 to 2.0 mol/mol collagen (Eyre *et al.*, 1988, Knott *et al.*, 1995, Masse *et al.*, 1996, Shiiba *et al.*, 2002) and a maximum total tripeptidyl value of 0.5 (Eyre *et al.*, 1988, Eyre *et al.*, 1984, Eyre & Oguchi, 1980, Knott *et al.*, 1995, Masse *et al.*, 1996, Shiiba *et al.*, 2001) are consistent with reports for bone from a variety of sources.

References for Supporting Information

- Acharya, A. S. & Sussman, L. G. (1984). *J. Biol. Chem.* **259**, 4372-4378.
- Bailey, A. J., Sims, J., Ebbesen, E. N., Mansell, J. P., Thomsen, J. S. & Mosekilde, L. (1999). *Calcif. Tissue Int.* **65**, 203-210.
- Banase, X., Sims, T. J. & Bailey, A. J. (2002). *J. Bone Miner. Res.* **17**, 1621-1628.
- Bella, J., Eaton, M., Brodsky, B. & Berman, H. M. (1994). *Science* **266**, 75-81.
- Berisio, R., Vitagliano, L., Mazzarella, L. & Zagari, A. (2002). *Protein Sci.* **11**, 262-270.
- Brodsky, B. & Persikov, A. V. (2005) *Adv. Protein Chem.* **70**, 301-339.
- Brodsky, B. & Shah, N. K. (1995). *FASEB J.* **9**, 1537-1546.
- Brown, E. M., King, G. & Chen, J. M. (1997). *J. Am. Leather Chem. Assoc.* **92**, 1-7.
- Burger, C., Zhou, H., Sics, I., Hsiao, B. S., Chu, B., Graham, L. & Glimcher, M. J. (2008). *Biophys. J.* **95**, 1985-1992.
- Chen, J. M., Kung, C. E., Fearheller, S. H. & Brown, E. M. (1991). *J. Protein Chem.* **10**, 535-552.
- Connolly, M. H. & Yelick, P. C. (2010). *J. Appl. Ichthyol.* **26**, 274-277.
- Dubois, G. M., Haftek, Z., Crozet, C., Garrone, R. & Le Guellec, D. (2002). *Gene* **294**, 55-65.
- Eyre, D. R. (1981) in *The Chemistry and Biology of Mineralized Connective Tissues*, edited by A. Veis, pp. 51-55. Amsterdam: Elsevier North Holland.
- Eyre, D. R. (1987). *Methods Enzymol.* **144**, 115-139.
- Eyre, D. R., Dickson, I. R. & Van Ness, K. (1988). *Biochem. J.* **252**, 495-500.
- Eyre, D. R., Koob, T. J. & Van Ness, K. P. (1984). *Anal. Biochem.* **137**, 380-388.
- Eyre, D. R. & Oguchi, H. (1980). *Biochem. Biophys. Res. Commun.* **92**, 403-410.
- Eyre, D. R. & Weis, M. A. (2013). *Calif. Tissue Int.* **93**, 338-347.
- Eyre, D. R., Weis, M. A., Hudson, D., Wu, J.-J. & Kim, L. (2011). *J. Biol. Chem.* **286**, 7732-7736.
- Fisher, S., Jagadeeswaran, P. & Halpern, M. E. (2003). *Dev. Biol.* **264** 64-76.
- Fratzl, P., Fratzl-Zelman, N. & Klaushofer, K. (1993). *Biophys. J.* **64**, 260-266.
- Glimcher, M. J. (1998) in *Metabolic Bone Disease and Clinically Related Disorders*, edited by L. V. Avioli & S. M. Krane, pp. 23-50. San Diego: Academic Press.
- Glimcher, M. J. (2006). *Rev. Mineral. Geochem.* **64**, 223-282.
- Hanson, D. A. & Eyre, D. R. (1996). *J. Biol. Chem.* **271**, 26508-26516.
- Katz, E. P. & Li, S. T. (1973). *J. Mol. Biol.* **73**, 351-369.
- Kivirikko, K. I., Myllyla, R. & Pihlajaniemi, t. (1989). *FASEB J.* **3**, 1609-1617.
- Knott, L. & Bailey, A. J. (1998). *Bone* **27**, 181-187.
- Knott, L., Whitehead, C. C., Fleming, R. H. & Bailey, A. J. (1995). *Biochem. J.* **310**, 1045-1051.
- Lee, D. D. & Glimcher, M. J. (1991). *J. Mol. Biol.* **217**, 487-501.
- Masse, P. G., Rimnac, C. M., Yamauchi, M., Cos, S. P., Coburn, P., Rucker, R. B., Howell, D. S. & Boskey, A. L. (1996). *Bone* **18**, 567-574.
- Mechanic, G. L., Banes, A. J., Henmi, M. & Yamauchi, M. (1985) in *The Chemistry and Biology of Mineralized Tissues*, edited by W. T. Butler, pp. 98-102. Birmingham, AL: EBSCO Media.

- Nagan, N. & Kagan, H. M. (1994). *J. Biol. Chem.* **269**, 22366-22371.
- Rho, J. Y., Mishra, S. R., Chung, K., Bai, J. & Pharr, G. M. (2001). *Ann. Biomed. Eng.* **29**, 1082-1088.
- Risteli, J., Tryggvason, K. & Kivirikko, K. I. (1977). *Eur. J. Biochem.* **73**, 485-492.
- Saito, M., Takenouchi, Y., Kunisaki, N. & Kimura, S. (2001). *Eur. J. Biochem.* **268**, 2817-2827.
- Shiiba, M., Arnaud, S. B., Tanazawa, H., Kitamura, E. & Yamauchi, M. (2002). *J. Bone Miner. Res.* **17**, 1639-1645.
- Shiiba, M., Arnaud, S. B., Tanzawa, H., Uzawa, K. & Yamauchi, M. (2001). *Conn Tiss Res* **42**, 303-311.
- Smith, J. (1968). *Nature* **219**, 157-158.
- Strausberg, R. L., Feingold, E. A., Grouse, L. H., Derge, J. G., Klausner, R. D., Collins, F. S., *et al.* (2002). *Proc. Natl. Acad. Sci. USA* **99**, 16899-16903.
- Terajima, M., Perdivara, I., Sricholpech, M., Deguchi, Y., Pleshko, N., Tomer, K. B. & Yamauchi, M. (2014). *J Biol Chem* **289**, 22998-23009.
- Woodhead-Galloway, J. & Machin, P. A. (1976). *Acta Crystallogr.* **A32**, 368-372.
- Yamauchi, M. & Sricholpech, M. (2012). *Essays Biochem.* **52**, 113-133.